Available online at www.sciencedirect.com
SCIENCE DIRECT®
PHYSICS LETTERS B
ELSEVIER
Physics Letters B 551 (2003) 49–55
www.elsevier.com/locate/npe

Helicity dependence of the $\vec{\gamma}\vec{p} \to n\pi^+\pi^0$ reaction in the second resonance region

GDH and A2 Collaborations

J. Ahrens [i], S. Altieri [o,p], J.R.M. Annand [f], G. Anton [c], H.-J. Arends [i], K. Aulenbacher [i], R. Beck [i], C. Bradtke [a], A. Braghieri [o], N. Degrande [d], N. d'Hose [e], H. Dutz [b], S. Goertz [a], P. Grabmayr [q], K. Hansen [h], J. Harmsen [a], D. von Harrach [i], S. Hasegawa [m], T. Hasegawa [k], E. Heid [i], K. Helbing [c], H. Holvoet [d], L. Van Hoorebeke [d], N. Horikawa [n], T. Iwata [m,1], O. Jahn [i], P. Jennewein [i], T. Kageya [n], B. Kiel [c], F. Klein [b], R. Kondratiev [l], K. Kossert [g], J. Krimmer [q], M. Lang [i], B. Lannoy [d], R. Leukel [i], V. Lisin [l], T. Matsuda [k], J.C. McGeorge [f], A. Meier [a], D. Menze [b], W. Meyer [a], T. Michel [c], J. Naumann [c], A. Panzeri [o,p], P. Pedroni [o], T. Pinelli [o,p], I. Preobrajenski [i,l], E. Radtke [a], E. Reichert [j], G. Reicherz [a], Ch. Rohlof [b], G. Rosner [f], T. Rostomyan [d], C. Rovelli [p], D. Ryckbosch [d], M. Sauer [q], B. Schoch [b], M. Schumacher [g], B. Seitz [g,2], T. Speckner [c], N. Takabayashi [m], G. Tamas [i], A. Thomas [i], R. van de Vyver [d], A. Wakai [n], W. Weihofen [g], F. Wissmann [g], F. Zapadtka [g], G. Zeitler [c]

[a] *Institut für Experimentalphysik, Ruhr-Universität Bochum, D-44801 Bochum, Germany*
[b] *Physikalisches Institut, Universität Bonn, D-53115 Bonn, Germany*
[c] *Physikalisches Institut, Universität Erlangen-Nürnberg, D-91058 Erlangen, Germany*
[d] *Subatomaire en Stralingsfysica, Universiteit Gent, B-9000 Gent, Belgium*
[e] *CEA Saclay, DSM/DAPNIA/SPhN, F-91191 Gif-sur-Yvette cedex, France*
[f] *Department of Physics & Astronomy, University of Glasgow, UK*
[g] *II Physikalisches Institut, Universität Göttingen, D-37073 Göttingen, Germany*
[h] *Department of Physics, University of Lund, Lund, Sweden*
[i] *Institut für Kernphysik, Universität Mainz, D-55099 Mainz, Germany*
[j] *Institut für Physik, Universität Mainz, D-55099 Mainz, Germany*
[k] *Faculty of Engineering, Miyazaki University, Miyazaki, Japan*
[l] *INR, Academy of Science, Moscow, Russia*
[m] *Department of Physics, Nagoya University, Chikusa-ku, Nagoya, Japan*
[n] *CIRSE, Nagoya University, Chikusa-ku, Nagoya, Japan*
[o] *INFN, Sezione di Pavia, I-27100 Pavia, Italy*
[p] *Dipartimento di Fisica Nucleare e Teorica, Università di Pavia, I-27100 Pavia, Italy*
[q] *Physikalisches Institut, Universität Tübingen, D-72076 Tübingen, Germany*

Received 27 August 2002; received in revised form 23 October 2002; accepted 11 November 2002

Editor: V. Metag

0370-2693/02
PII: S0370-2693(02)03008-3

Abstract

The helicity dependence of the total cross section for the $\vec{\gamma}\vec{\mathrm{p}} \to \mathrm{n}\pi^+\pi^0$ reaction has been measured for the first time at incident photon energies from 400 to 800 MeV. The measurement was performed with the large acceptance detector DAPHNE at the tagged photon beam facility of the MAMI accelerator in Mainz. This channel is found to be excited predominantly when the photon and proton have a parallel spin orientation, due to the intermediate production of the D_{13} resonance.

1. Introduction

The excitation spectrum of the nucleon has been the subject of many experimental and theoretical studies over the years. A precise knowledge of the properties of the nucleon resonances is a prerequisite for a complete understanding of the nucleon itself. Among the tools best suited to study these properties are pion production processes in both electromagnetic (γN, γ^*N) and hadronic (πN) reactions. A large data set, mainly for single pion production, combined with extensive partial-wave analyses and theoretical models has provided valuable information such as the Breit–Wigner masses, decay widths, and decay amplitudes for numerous resonances (e.g., P_{33}, S_{11}, $D_{13}, \ldots$). In several cases, however, the precision with which the resonance properties are known is still rather poor [1]. This is especially true for the higher lying and strongly overlapping resonances that couple more weakly to the photon and show up in the double pion production region.

Since the resonance properties are helicity dependent, valuable new input to disentangle and study these resonances is provided by the helicity dependence of double pion photoproduction using polarized beams and polarized targets.

As a by-product, the measurement of the helicity dependence of the N$\pi\pi$ channels will give a deeper insight into the dynamics contributing to the Gerasimov–Drell–Hearn (GDH) sum rule for the nucleon [2,3]. This sum rule is given by:

$$\int_{\nu_0}^{\infty} \frac{\sigma_{3/2} - \sigma_{1/2}}{\nu}\,\mathrm{d}\nu = \frac{2\pi^2\alpha}{m_{\mathrm{N}}^2}\kappa_{\mathrm{N}}^2,$$

where ν is the photon energy and ν_0 is the pion production threshold. α is the fine structure constant, m_{N} is the mass and κ_{N} is the anomalous magnetic moment of the nucleon. The cross sections $\sigma_{1/2}$ and $\sigma_{3/2}$ are for the absorption of circularly polarized photons by longitudinally polarized nucleons, with anti-parallel and parallel relative spin orientations, respectively. We have recently published [4] the first experimental results for the proton on the total photoabsorption cross section difference ($\sigma_{3/2} - \sigma_{1/2}$) up to 800 MeV.

A thorough understanding of the GDH integral also requires a knowledge of the contributions of the partial photoproduction channels, and our results [4] show that double pion photoproduction is important. Large differences exist among the few estimates that have been made for the double pion channels on the basis of various theoretical models. For instance, Karliner [5] predicts 65 μb, Coersmeier [6] gives 83 μb and the UIM calculation [7] predicts 22 μb.

As a part of our experimental study of the helicity dependence of the double pion photoproduction reactions on the proton, we present here the first data on the $\vec{\gamma}\vec{\mathrm{p}} \to \mathrm{n}\pi^+\pi^0$ process. An improved theoretical description of this reaction channel, in which the underlying processes are presently not fully understood, is an extra motivation for this investigation. After the early work by Lüke and Söding [8], Nacher and Oset [9] (with an extension of the Tejedor and Oset model [10]) and Murphy and Laget [11] have developed models to describe the double pion production channels. They evaluate the main elementary mechanisms contributing to these reactions in the framework of an effective Lagrangian model. Both models include non-resonant Born terms and resonant terms but they do not completely agree on the issue of which resonances predominate.

A different approach (RPR), based on t-channel Regge exchanges, is also being developed at present [12,13]. The (π and ρ) t-channel Regge exchanges

E-mail address: pedroni@pv.infn.it (P. Pedroni).

[1] Permanent address: Yamagata University, Japan.

[2] Present address: II Physikalisches Institut, Universität Gießen, Gießen, Germany.

provide a good description of the energy and t dependence of the $\gamma N \to \pi\Delta$ reaction for $E_\gamma > 2$ GeV [12]. At lower energies, the model is complemented by adding resonant s-channel D_{13} excitation.

2. Experimental setup

The present data were obtained as a part of the GDH experiment at MAMI, Mainz. For a detailed description of the experimental apparatus, we refer to [4,14] and references therein.

Circularly polarized photons were obtained by Bremsstrahlung of longitudinally polarized electrons having an average polarization of 75% [15]. The electron polarization was continuously measured using a Møller polarimeter [16] with an accuracy of 3%. The Bremsstrahlung photons were tagged using the Glasgow–Mainz spectrometer with an energy resolution of about 2 MeV [17]. The tagging efficiency (probability of a photon passing through the collimation system given an electron hit the spectrometer focal plane detector) was monitored throughout the experiment by an e^+e^- detector with an accuracy of 2%.

Longitudinally polarized protons were provided by a frozen-spin target [18] using butanol (C_4H_9OH) as target material. A maximum polarization of 90% was reached, with a relaxation time of about 200 hours. The target polarization was monitored, with an accuracy of 1.6%, using NMR techniques.

The central detector was DAPHNE [19], a charged particle tracking detector with cylindrical symmetry. It covers the full azimuthal angular region and polar angles θ_{lab} from 21° to 159°. An outer scintillator–absorber sandwich allowed the detection of neutral pions with reasonable efficiency. In order to extend the forward angle coverage, the central detector was complemented by the MIDAS [20], STAR and FFW [21] systems. Since electromagnetic background is large in forward directions, a N_2-aerogel Čerenkov detector [22] was installed to veto this unwanted background.

3. Data analysis

The data analysis of the $\vec{\gamma}\vec{p} \to n\pi^+\pi^0$ process was performed in two parts. In the first the analysis method was developed and verified using calibration data taken with an unpolarized photon beam and a pure hydrogen target. In the second the same method was used with the polarized data. For the results presented here, only the central DAPHNE detector has been used. A detailed discussion of the analysis is given in Ref. [12].

As in Ref. [23], events from the $n\pi^+\pi^0$ reaction are selected by the detection of the π^+ and π^0 in coincidence since the contribution of reactions with more than two pions in the final state is negligible within the measured photon energy range.

The charged pion is identified using a combination of the range method described in Ref. [24] and a $\Delta E - E$ technique [12]. The range method uses the charged particle energy losses in all traversed DAPHNE scintillator layers to discriminate between protons and charged pions (with a systematic misidentification error of 2%) and to determine their kinetic energy. Since this procedure can only be used for particles that are stopped in the detector, the identification of charged pions that have sufficient energy to escape the detector is performed by comparing information provided by the geometrical path of the particle inside the detector with the energy deposited in the thickest scintillator layer, which has the best energy resolution. An example of the spectra obtained in such a case is shown in Fig. 1. Two bands, corresponding respectively to $\pi^\pm$ and protons can be clearly seen.

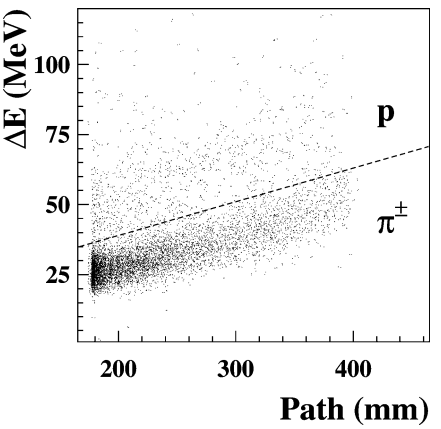

Fig. 1. The energy released in the thickest (10 cm) scintillator layer of DAPHNE by particles that escaped the detector is shown as a function of their geometrical path (in equivalent scintillator thickness) inside the detector.

However, quasi-relativistic protons having a momentum higher than $\simeq 900$ MeV/c are not distinguishable from charged pions. Simulations show that this causes, at the higher measured photon energies, a contamination of about 5% to the $n\pi^+\pi^0$ channel due to the $p\pi^0$ reaction [12], which is subtracted as discussed below.

A π^0 can be identified by the coincident detection of its two decay photons as described in Ref. [23]. However, in order to maximize the detection efficiency in the present measurement and thus improve the statistical precision, events in which only one photon was detected were also analyzed. The π^0 detection efficiency (ϵ_{π^0}) was calculated with a GEANT based simulation which models accurately the geometry and composition of the GDH detector setup and accounts for electronic thresholds. The resulting efficiency for single photon detection is a smoothly rising function of the photon energy with a maximum value of about 60%. This is a considerable increase compared to an average efficiency of about 20% when both decay photons are required [23].

A check on the validity of the simulation was obtained by comparing the simulated efficiency for the $\gamma p \to p\pi^0$ channel with an efficiency measurement at photon energies where the effect of the $N\pi\pi$ processes can be neglected. Under this condition, ϵ_{π^0} is equal to the fraction of the events with a proton in the final state that have also one or more photons in coincidence. The result of this comparison is shown in Fig. 2 where the two dashed lines represent the maximum and minimum efficiency values obtained from the estimated systematic error of the simulation (4% of ϵ_{π^0}). The good agreement between the $\gamma p \to p\pi^0$ simulation and experiment gives confidence in the simulated efficiencies for the $n\pi^+\pi^0$ process.

The disadvantage of basing the π^0 identification on single photon detection is the increased background. This calls for a more elaborate treatment of the background processes. For instance, events from the $\gamma p \to n\pi^+$ reaction can be misidentified as $n\pi^+\pi^0$ events when a secondary particle is emitted after a hadronic interaction of the π^+ or neutron inside DAPHNE materials.

The different background contributions have been evaluated by means of the GEANT simulation. The total background amounts to about 40% of the measured $n\pi^+\pi^0$ yield at 500 MeV and to 15% at 750 MeV in the case of the unpolarized cross section. The background simulation is checked by comparing the measured unpolarized yield with the yield obtained when requiring two decay photons for the π^0 identification. In the latter case the background is negligible and the statistical precision is still good enough to make a significant comparison. This comparison is shown in Fig. 3. The good agreement supports the background procedure used. On the basis of the observed differences, the systematic error in the $n\pi^+\pi^0$ cross section evaluation due to the background subtraction, is estimated to be at most 3%.

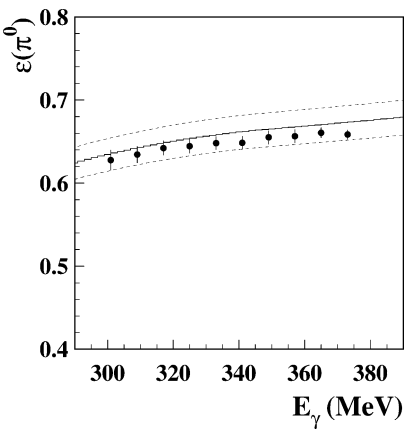

Fig. 2. Comparison between the simulated (solid line) and measured (solid circles) π^0 detection efficiency (ϵ_{π^0}) in the $\gamma p \to p\pi^0$ process as a function of photon energy. The dashed lines represent the estimated systematic error band of the simulation (4% of ϵ_{π^0}).

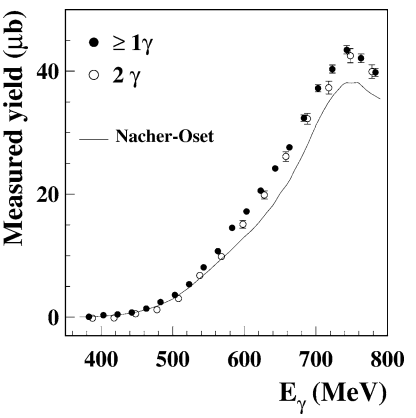

Fig. 3. Measured yield of the $\gamma p \to n\pi^+\pi^0$ channel obtained when the π^0 is identified by requiring two photons in coincidence (open circles) or by at least one photon (full circles). The solid line represents the prediction of the Nacher–Oset model [9].

In Fig. 3, the results of the Nacher–Oset model calculation [9] subjected to the experimental detector acceptance are also shown. Given the fairly good agreement with the data, the contribution of particles produced outside the detector angular and momentum acceptance (about 20% of the measured yield over most of the measured photon energy range) was evaluated using this model. A difference in the extrapolation of at most 10% was found when a uniform 3-body phase space distribution was assumed instead of the model. This difference gives an estimated systematic error of 2% of the evaluated total cross section due to this extrapolation.

The resulting total unpolarized cross section σ_{tot} is shown in Fig. 4 and compared to previous DAPHNE [23] and TAPS [25] data and to the predictions of the Nacher–Oset and RPR models. The addition in quadrature of all the different sources of systematic errors gives an overall systematic error of 6% of σ_{tot}. As described in Ref. [12], the previous DAPHNE data contain a systematic error due to an imprecise solid angle correction for the finite target length. The excellent agreement with TAPS data indicates that the estimated systematic error is an upper limit.

The same analysis method has been applied to the doubly polarized data to obtain the difference between the helicity cross sections $\sigma_{1/2}$ and $\sigma_{3/2}$. The difference is taken to cancel the background from the unpolarized carbon and oxygen nuclei in the butanol target [26].

An extrapolation based on the Nacher–Oset model for the $(\sigma_{3/2} - \sigma_{1/2})$ difference has also been used to account for out-of-acceptance particles even if the agreement with our data is not as good as in the unpolarized case. Extrapolations given by the RPR model and phase space are very similar to the extrapolation that we used, with a maximum difference of 10% in the correction. For this reason, the estimated systematic error in the extrapolation is assumed to be the same as in the unpolarized case.

4. Results and comments

The resulting helicity dependent cross section difference $(\sigma_{3/2} - \sigma_{1/2})$ is presented in Fig. 5 together with the predictions of the Nacher–Oset and RPR models. The systematic error on this difference is increased compared to the unpolarized case due to the uncertainties in the beam and target polarization values. We estimate the total systematic error to be 7% of the measured cross section difference $(\sigma_{3/2} - \sigma_{1/2})$.

Two features stand out in Fig. 5. The difference $(\sigma_{3/2} - \sigma_{1/2})$ is positive, which implies that the 3/2 intermediate spin state is dominant in the $n\pi^+\pi^0$ production process. Furthermore, an indication of a peak around 750 MeV is observed. By combining this result with the unpolarized cross section, the separation between the $\sigma_{1/2}$ and $\sigma_{3/2}$ helicity cross sections, which

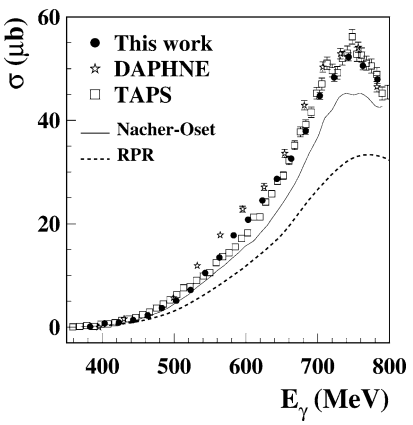

Fig. 4. The total unpolarized cross section for the $\gamma p \to n\pi^+\pi^0$ channel obtained in this work is compared to previous DAPHNE [23] and TAPS [25] data. The solid and dashed lines represent the prediction of the Nacher–Oset [9] and the RPR [12,13] models, respectively. Only statistical errors are shown.

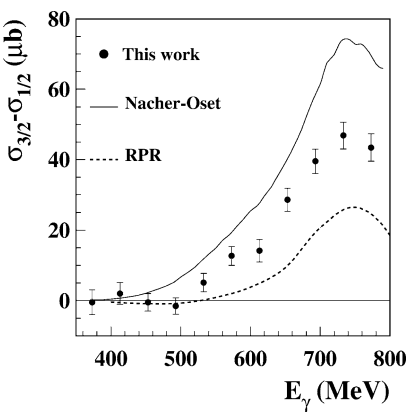

Fig. 5. Helicity dependent cross section difference $(\sigma_{3/2} - \sigma_{1/2})$ for the $\vec{\gamma}\vec{p} \to n\pi^+\pi^0$ reaction. Curves as in the previous figure. Only statistical errors are shown.

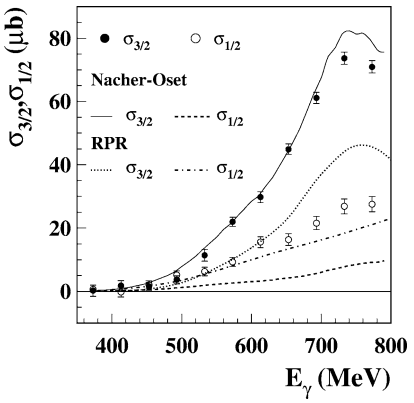

Fig. 6. The helicity dependent cross sections $\sigma_{1/2}$ (open circles) and $\sigma_{3/2}$ (full circles) for the $\vec{\gamma}\vec{\mathrm{p}} \to \mathrm{n}\pi^+\pi^0$ channel are compared to the predictions of the Nacher–Oset [9] and RPR [12,13] models.

are experimentally not directly accessible, can also be extracted. The resulting values for $\sigma_{1/2}$ and $\sigma_{3/2}$ are given in Fig. 6 together with the predictions of the Nacher–Oset and RPR models.

According to Refs. [9,13], the D_{13} resonance is largely responsible for the observed dominance and shape of the $\sigma_{3/2}$ cross section, via the processes $\gamma\mathrm{N} \to D_{13} \to \pi\Delta \to \pi\pi\mathrm{N}$ and $\gamma\mathrm{N} \to D_{13} \to \rho\mathrm{N} \to \pi\pi\mathrm{N}$. The latter mechanism gained extra attention since indications for its presence were found in invariant mass distributions measured by the TAPS Collaboration for the $\gamma\mathrm{p} \to \mathrm{n}\pi^+\pi^0$ reaction [25] and with DAPHNE for the isospin-symmetric reaction $\gamma\mathrm{n} \to \mathrm{p}\pi^-\pi^0$ reaction [27]. However, as can be seen in Fig. 6, we also observe a non-negligible $\sigma_{1/2}$ cross section, which points to mechanisms not involving the D_{13} resonance, such as $\gamma\mathrm{N} \to \pi\Delta \to \pi\pi\mathrm{N}$ and $\gamma\mathrm{N} \to \rho\mathrm{N} \to \pi\pi\mathrm{N}$. These latter mechanisms are not fully accounted for by the Nacher–Oset model, which gives a good description of the $\sigma_{3/2}$ data, but falls significantly below the data for $\sigma_{1/2}$. On the contrary $\sigma_{1/2}$ is much better reproduced by the RPR approach, which at the same time underestimates the $\sigma_{3/2}$ cross section.

The contribution of the $\gamma\mathrm{p} \to \mathrm{n}\pi^+\pi^0$ channel to the GDH sum rule in the covered photon energy range from threshold up to 800 MeV is found to be $(11.3 \pm 0.7 \pm 0.7)$ μb (statistical and systematical errors, respectively). This particular channel provides a non-negligible fraction ($\simeq 5.5\%$) of the total GDH sum rule value (205 μb) and, as is clear from Fig. 5, this contribution is not saturated within the measured energy interval. The contribution of this channel to the forward spin polarizability γ_0 amounts to 3%.

5. Conclusion

The first measurement of the helicity dependence of the total cross section for the $\vec{\gamma}\vec{\mathrm{p}} \to \mathrm{n}\pi^+\pi^0$ reaction has been carried out at incident photon energies from 400 to 800 MeV within the context of the GDH experiment at MAMI. A strong helicity dependence is observed, with clear dominance of the $\sigma_{3/2}$ over the $\sigma_{1/2}$ cross section, which moreover suggests resonant behaviour due to the intermediate excitation of the D_{13} resonance. These results provide valuable new input for the determination of the D_{13} resonance properties and for the theoretical models and partial wave analyses of the photoproduction processes.

Acknowledgements

The authors wish to acknowledge the excellent support of the accelerator group of MAMI. They also thank E. Oset and M. Vanderhaeghen for the latest results of their calculations. This work was supported by the Deutsche Forschungsgemeinschaft (SFB 201, SFB 443 Schwerpunktprogramm 1034 and GRK683), the INFN–Italy, the FWO Vlaanderen–Belgium, the IWT–Belgium, the UK Engineering and Physical Science Research Council, the DAAD, and the Grant-in-Aid, Monbusho, Japan.

References

[1] D.E. Groom, et al., Eur. Phys. J. C 15 (2000) 1.
[2] S.B. Gerasimov, Sov. J. Nucl. Phys. 2 (1966) 430.
[3] S.D. Drell, A.C. Hearn, Phys. Rev. Lett. 16 (1966) 908.
[4] J. Ahrens, et al., Phys. Rev. Lett. 87 (2001) 022003.
[5] I. Karliner, Phys. Rev. D 7 (1973) 2717.
[6] I. Coersmeier, Diplomarbeit, University of Bonn, 1993.
[7] D. Drechsel, et al., Nucl. Phys. A 645 (1999) 145.
[8] D. Lüke, P. Söding, in: Springer Tracts in Modern Physics, Vol. 59, Springer-Verlag, 1971, p. 39.
[9] J.C. Nacher, E. Oset, Nucl. Phys. A 697 (2002) 372; J.C. Nacher, et al., Nucl. Phys. A 695 (2001) 295.

[10] J.A. Tejedor, E. Oset, Nucl. Phys. A 571 (1994) 667.
[11] L.Y. Murphy, J.M. Laget, Report DAPNIA-SPHN-95-42, 1995.
[12] H. Holvoet, PhD thesis, University of Gent, 2001.
[13] H. Holvoet, M. Vanderhagen, in preparation.
[14] M. MacCormick, et al., Phys. Rev. C 55 (1996) 41.
[15] K. Aulenbacher, Nucl. Instrum. Methods A 391 (1997) 498.
[16] I. Preobajenski, PhD thesis, University of Mainz, 2001.
[17] I. Anthony, et al., Nucl. Instrum. Methods A 301 (1991) 230; S.J. Hall, et al., Nucl. Instrum. Methods A 368 (1996) 698.
[18] C. Bradtke, et al., Nucl. Instrum. Methods A 436 (1999) 430.
[19] G. Audit, et al., Nucl. Instrum. Methods A 301 (1991) 473.
[20] S. Altieri, et al., Nucl. Instrum. Methods A 452 (2000) 185.
[21] M. Sauer, et al., Nucl. Instrum. Methods A 378 (1996) 146.
[22] B. Lannoy, PhD thesis, University of Gent, 2000.
[23] A. Braghieri, et al., Phys. Lett B 363 (1995) 46.
[24] A. Braghieri, et al., Nucl. Instrum. Methods A 343 (1994) 623.
[25] W. Langgärtner, et al., Phys. Rev. Lett. 87 (2001) 052001.
[26] J. Ahrens, et al., Phys. Rev. Lett. 84 (2000) 5950.
[27] A. Zabrodin, et al., Phys. Rev. C 60 (1999) 055201.